INSTITUTE OF PHYSICS PUBLISHING JOURNAL OF PHYSICS: CONDENSED MATTER

J. Phys.: Condens. Matter **16** (2004) S4159–S4168 PII: S0953-8984(04)79811-2

# Capillary evaporation in colloid–polymer mixtures selectively confined to a planar slit

**Matthias Schmidt**[1], **Andrea Fortini and Marjolein Dijkstra**

Soft Condensed Matter, Debye Institute, Utrecht University, Princetonplein 5, 3584 CC Utrecht, The Netherlands

Received 26 April 2004
Published 10 September 2004
Online at stacks.iop.org/JPhysCM/16/S4159
doi:10.1088/0953-8984/16/38/029

**Abstract**

Using density functional theory and Monte Carlo simulations we investigate the Asakura–Oosawa–Vrij mixture of hard sphere colloids and non-adsorbing ideal polymers under selective confinement of the colloids to a planar slab geometry. This is a model for confinement of colloid–polymer mixtures by either two parallel walls with a semi-permeable polymer coating or through the use of laser tweezers. We find that such a pore favours the colloidal gas over the colloidal liquid phase and induces capillary evaporation. A treatment based on the Kelvin equation gives a good account of the location of the capillary binodal for large slit widths. The colloid density profile is found to exhibit a minimum (maximum) at contact with the wall for large (small) slit widths.

## 1. Introduction

Capillary evaporation denotes the situation where a confining pore is filled with a gas in equilibrium with its bulk liquid phase. The phenomenon is an antagonist of capillary condensation, where the pore instead stabilizes the liquid phase that in turn is in equilibrium with the bulk gas phase [1, 2]. Which of the two scenarios will occur for a given fluid depends on the nature of the confinement and in particular on the interaction between the fluid particles and the pore walls. Despite the fundamental analogy, capillary evaporation has only recently attracted more attention, in particular for the Lennard-Jones fluid, which was studied theoretically and with simulation, capillary evaporation being observed for purely repulsive walls (and capillary condensation for attractive walls) [3–5].

Colloid–polymer mixtures are mesoscopic model systems that enable one to study fundamental issues in condensed matter [6]. The Asakura–Oosawa–Vrij (AOV) model [7, 8] of hard sphere colloids and ideal polymers is a simple model that has been studied extensively using theory [9–13] and simulation [11, 14–18]. The presence of polymers induces an effective

[1] On leave from: Institut für Theoretische Physik II, Heinrich-Heine-Universität Düsseldorf, Universitätsstraße 1, D-40225 Düsseldorf, Germany.

  

attraction between colloids driving, for high enough polymer concentration and large enough colloid-to-polymer size ratio, a (colloidal) gas–liquid phase transition in bulk [7–10]. The same (depletion) effect leads to an attraction between a single colloidal particle and a planar hard wall (that is impenetrable to both colloids and polymers) [19]. Much attention has been devoted to the wetting of a (single) wall by the colloidal liquid as studied theoretically [20–24] and by means of simulations [14] and experiments [22, 25–27].

We have recently investigated capillary condensation of the AOV mixture confined between two parallel hard walls. Corresponding experimental set-ups can be well controlled due to their relatively large (as compared to molecular fluids) intrinsic length scales of the order of $\sim$100 nm particle diameter [22, 27, 28]. Furthermore, surface corrugations of the confining walls are of minor importance as (glass) substrates are practically smooth on the colloidal length scale. Our results from Monte Carlo (MC) simulations and density functional theory (DFT) indicate that capillary condensation does occur. That purely repulsive walls lead to such behaviour might seem surprising at first glance. However, although the bare interaction between the wall and the two species is purely repulsive, the concept of integrating out degrees of freedom, in this case those of the polymers, permits us to relate the properties of the binary mixture to those of a corresponding one-component fluid (of colloids) interacting through an effective one-component Hamiltonian which consists of effective many-body interactions. The dominant term in this effective many-body Hamiltonian is the so-called depletion pair potential, which is known to be attractive. Via the same mechanism an effective attraction between the colloid and hard wall arises [19] as the dominant term for the effective polymer-mediated wall–colloid interaction. This gives a qualitative explanation of the occurrence of capillary condensation between parallel hard walls. However, care should be taken, as previous work [14, 20, 21, 24] showed that the effective higher-body interactions (repulsive and attractive) change the bulk phase behaviour and adsorption phenomena substantially from those found for pairwise simple fluids; e.g. an anomalously large bulk liquid regime is found and, far from the bulk triple point, several layering transitions in the partial wetting regime prior to a transition to complete wetting by colloidal liquid are found.

In this work, we consider two parallel semi-permeable walls that do not generate an effective wall–colloid attraction. The polymers are unconfined and can penetrate the walls which act solely on the colloids. Such situations have been investigated before for random sphere matrices [29] and for a single wall [23]. There are two possible experimental realizations for selective confinement between two planes:

(i) A polymer-coated brush that is impenetrable to colloids but penetrable to polymers [26].
(ii) Confinement of colloids via an appropriate set-up of laser tweezers to a thin sheet in space.

The paper is organized as follows. In section 2 we define the model explicitly and give an overview of the DFT and MC techniques used. In section 3 results are presented and concluding remarks are given in section 4.

## 2. Model and methods

The AOV model is a mixture of colloidal hard spheres (species c) of diameter $\sigma_c$ and ideal polymers (species p) of diameter $\sigma_p$ interacting with pair interactions $V_{ij}(r)$ between species $i, j = c, p$ as a function of the centre–centre distance. The colloid–colloid interaction is that of hard spheres: $V_{cc}(r) = \infty$ if $r < \sigma_c$ and zero otherwise. Polymers and colloids also behave as hard spheres: $V_{cp}(r) = \infty$ if $r < (\sigma_c + \sigma_p)/2$ and zero otherwise. The polymers are assumed to be non-interacting: $V_{pp}(r) = 0$ for all distances.

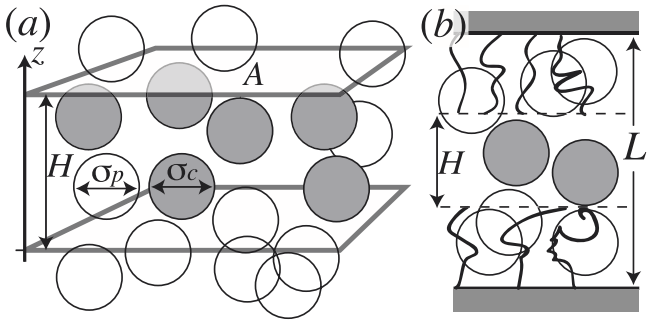


**Figure 1.** An illustration of the selectively confined AOV model of colloidal hard spheres (grey) and polymers (white). (a) The confinement is such that the volume accessible to the colloids is between two parallel planes at distance $H$. Polymers do not experience confinement. (b) The confinement between parallel substrates (grey) at distance $L$ coated with a polymer brush (wiggles). The free distance between the two polymer brushes is $H$; soluted polymers (open spheres) are able to penetrate the brush but not the substrate; the brush acts like a hard wall for colloids.

We consider a confining external potential acting solely on the colloids:

$$V_{\mathrm{ext,c}}(z) = \begin{cases} 0 & \sigma_{\mathrm{c}}/2 < z < H - (\sigma_{\mathrm{c}}/2), \\ \infty & \text{otherwise}, \end{cases} \tag{1}$$

where $z$ is the space coordinate perpendicular to the confining walls. There is no external potential acting on the polymer, i.e. formally $V_{\mathrm{ext,p}} = 0$. See figure 1(a) for an illustration of the model. Note that any substrate that supports the polymer coating will be decoupled from the system due to the ideality of polymers provided that the separation distance between the two substrate walls is $L > H + 2\sigma_{\mathrm{p}}$ (see figure 1(b) for an illustration).

As control parameters we use the packing fractions $\eta_i = \pi\sigma_i^3\rho_i/6$, where $\rho_i = N_i/(AH)$ is the number density of species $i = \mathrm{c}, \mathrm{p}$; $N_i$ is the number of particles and $A$ is the lateral area of the system (perpendicular to the $z$-direction). Furthermore, we use the packing fraction in a pure reservoir of polymers, $\eta_{\mathrm{p}}^{\mathrm{r}}$, that is in chemical equilibrium with the system.

The methods that we employ to study this model are very similar to those in a previous study of capillary condensation [30], hence we will give here only a brief overview. To obtain DFT results we use the excess free energy functional of [12, 13] that is an extension of Rosenfeld's fundamental measure theory for hard sphere mixtures [31] to the AOV model. Results for density profiles and phase behaviour are obtained by minimizing numerically the grand potential functional. Furthermore, we use the Gibbs ensemble Monte Carlo (MC) simulation method [32, 33], where both the structure and the phase behaviour are directly accessible. Fugacities are calculated via the test particle insertion procedure [34]. For more technical details of both approaches we refer the reader directly to [30].

## 3. Results

We first display results for the fluid demixing part of the bulk phase diagram in figure 2 as a function of the colloid packing fraction, $\eta_{\mathrm{c}}$, and polymer reservoir packing fraction, $\eta_{\mathrm{p}}^{\mathrm{r}}$. In the unconfined (bulk) situation, which we recover formally for infinite plate separation distances $H/\sigma_{\mathrm{c}} \to \infty$, the DFT result reduces to that of free volume theory which is known to be accurate far away from the critical point [14–16], but it underestimates the critical value of $\eta_{\mathrm{p}}^{\mathrm{r}}$. Our results confirm this finding. For decreasing values of $H/\sigma_{\mathrm{c}}$ the binodal shifts significantly to higher values of $\eta_{\mathrm{p}}^{\mathrm{r}}$. The shift of the critical point to higher $\eta_{\mathrm{p}}^{\mathrm{r}}$ corresponds to the common

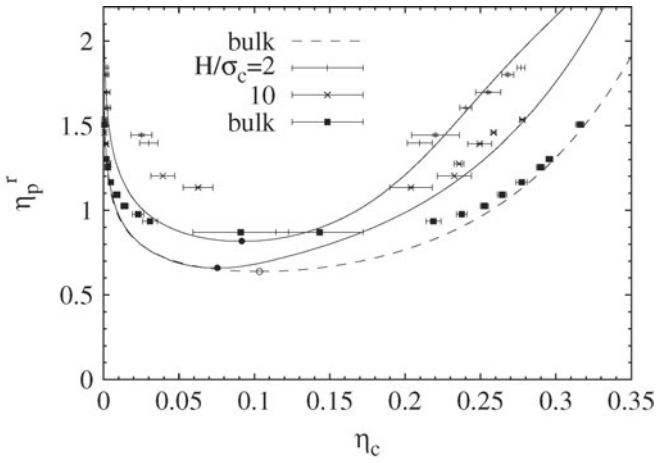


**Figure 2.** The phase diagram of the AOV model confined between depletionless walls as a function of the colloid packing fraction, $\eta_c$, and polymer reservoir packing fraction, $\eta_p^r$, for plate separation distances $H/\sigma = \infty$ (bulk), 10, 2 and size ratio $q = 1$. Shown are results from simulations (symbols) and DFT (solid curves). The bulk binodal from DFT is identical to that from free volume theory (dashed curve).

shift to smaller temperatures (i.e. larger inverse temperatures) in simple substances. As the attraction between the colloids is diminished due to the confinement, more polymer, yielding a stronger attractive depletion interaction between the colloids, is needed to drive the phase separation. For $L/\sigma_c = 10$ the liquid branch of the binodal shifts to considerably smaller values of $\eta_c$, similarly to the case of capillary condensation between parallel hard walls. As we will demonstrate below, when investigating structure in detail, this shift is accompanied with the growth of colloidal gas films on both walls. Close to the critical point the coexistence values of $\eta_c$ in the capillary gas phase predicted by the two approaches deviate significantly from each other, i.e. the simulation results indicate larger values of $\eta_c$ as compared to the theoretical calculation. This deviation is consistent with the (again) too high critical value of $\eta_p^r$ from DFT as compared to the simulation results. Also the (estimated) critical value of $\eta_c$ is higher in simulation than in theory.

We also plot the same phase diagram as a function of the scaled colloid chemical potential $\beta\mu_c = \ln(z_c\sigma_c^3)$, where $z_c$ is the colloid fugacity, and the polymer reservoir packing fraction, $\eta_p^r$, in figure 3. It is apparent that the binodals for the confined system are shifted towards higher values of $\ln(z_c\sigma_c)$, the shift being small for $H/\sigma_c = 10$ but considerable for $H/\sigma_c = 2$. This trend implies that state points between the bulk binodal and the binodal of the confined system (and for values of $\eta_p^r$ larger than either critical point) describe bulk liquid states in coexistence with gas states inside the capillary, clearly signalling capillary evaporation. The agreement between results from simulation and theory is quantitative except for the aforementioned difference in the location of the critical point.

As an alternative, simple treatment we use the Kelvin equation and restrict ourselves to the application of its one-component version, i.e. keeping the polymer reservoir packing fraction fixed. Previous density functional theory calculations showed complete drying everywhere along the liquid branch of the binodal [23] and, thus, $\gamma_{lg} = \gamma_{wl} - \gamma_{wg}$, where $\gamma_{lg}$, $\gamma_{wl}$ and $\gamma_{wg}$ are the interface tensions between liquid gas, wall liquid and wall gas, respectively. The shift in colloid chemical potential $\Delta\mu_c$ due to the confinement reads

$$\Delta\mu_c = \frac{2\gamma_{lg}}{(\rho_c^l - \rho_c^g)(H - \sigma_c)}, \tag{2}$$

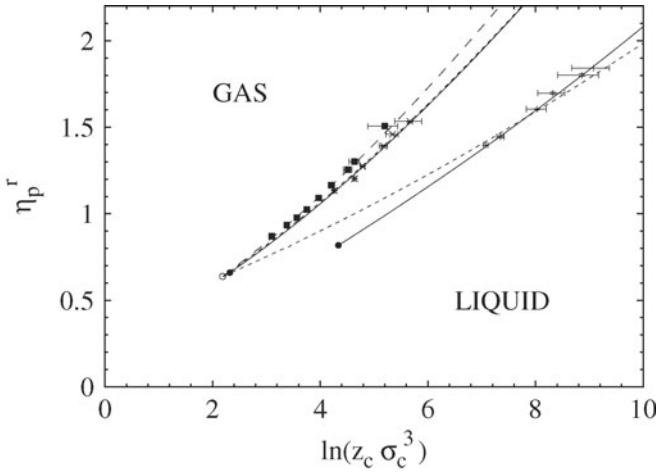


**Figure 3.** The same as figure 2, but as a function of the colloid chemical potential, $\ln(z_c\sigma_c^3)$, and polymer reservoir packing fraction, $\eta_p^r$. Also shown are the results from the Kelvin equation (short dashed curves) using the gas–liquid interface tension, $\gamma_{lg}$, obtained from DFT as an input.

$\rho_c^l$ ($\rho_c^g$) is the number density of the coexisting liquid (gas) bulk phase. $\Delta\mu_c = \mu_c^{evap} - \mu_c^{coex} > 0$ indicates capillary evaporation, where $\mu_c^{evap}$ denotes the chemical potential at the capillary binodal and $\mu_c^{coex}$ that at the bulk liquid binodal. We use DFT results for $\gamma_{lg}$ and display the corresponding binodals in figure 3. For $H/\sigma_c = 10$ the result is (except very close to the critical point) practically identical to the result from the full numerical DFT calculation. Even for the strongly confined system of $H/\sigma_c = 2$ the binodal is reproduced reasonably, albeit with a (typical) slope that is too small in the $(\ln(z_c\sigma_c^3), \eta_p^r)$ plane. We emphasize that we use a slab thickness reduced by one particle diameter, $H - \sigma_c$, in the Kelvin equation (2). Commonly, the bare value $H$ is used, which we find to give far inferior results for the strongly confined system, $H/\sigma_c = 2$, i.e. a much too small magnitude of $\Delta\mu_c$. This behaviour is consistent with that found for capillary condensation of the AO model between parallel hard walls [30]. There it was argued that the dimensional crossover to the two remaining spatial dimensions upon approaching $H \to \sigma_c$ induces a divergence, which is correctly captured by a form similar to that of equation (2). The only prominent deficiency of the results from the Kelvin equation is the false prediction that the capillary critical point is identical to the bulk critical point.

We also display our results as a function of the colloid packing fraction of a bulk reservoir of the colloid–polymer mixture, $\eta_c^{bulk}$, which is in equilibrium with the confined system. As a second parameter we keep $\eta_p^r$. The topology of the resulting phase diagram, as displayed in figure 4, resembles closely that of a simple substance with capillary evaporation binodals running as lines along the liquid branch of the bulk binodal. The shift of the capillary evaporation binodals with respect to the bulk liquid binodal is larger for stronger confinement. The prediction from the Kelvin equation (not shown) is very close to the DFT result for $H/\sigma_c = 10$, but differs somewhat (similar to the difference in observed in figure 3) for $H/\sigma_c = 2$. As illustrations we display snapshots of coexisting states obtained from MC simulation in figure 5.

We also investigate density profiles of both species inside the slit pore; see figure 6 for MC and DFT results for $H/\sigma_c = 10$. In order to compare results from the two approaches, we take equal values of $\eta_p^r$ at (capillary) coexistence. Sufficiently far away from the critical point, for $\eta_p^r = 1.39$—see figure 6(a)—the gas phase is practically an ideal gas of polymers without any colloids. The colloid density profile in the liquid phase is flat in the middle of

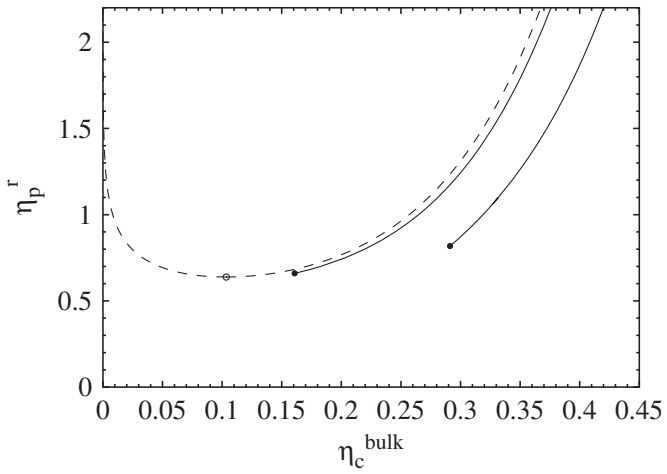


**Figure 4.** The same as figure 3, but as a function of the colloid packing fraction in the coexisting bulk mixture, $\eta_c^{bulk}$, and the polymer reservoir packing fraction, $\eta_p^r$. Shown are results from DFT.

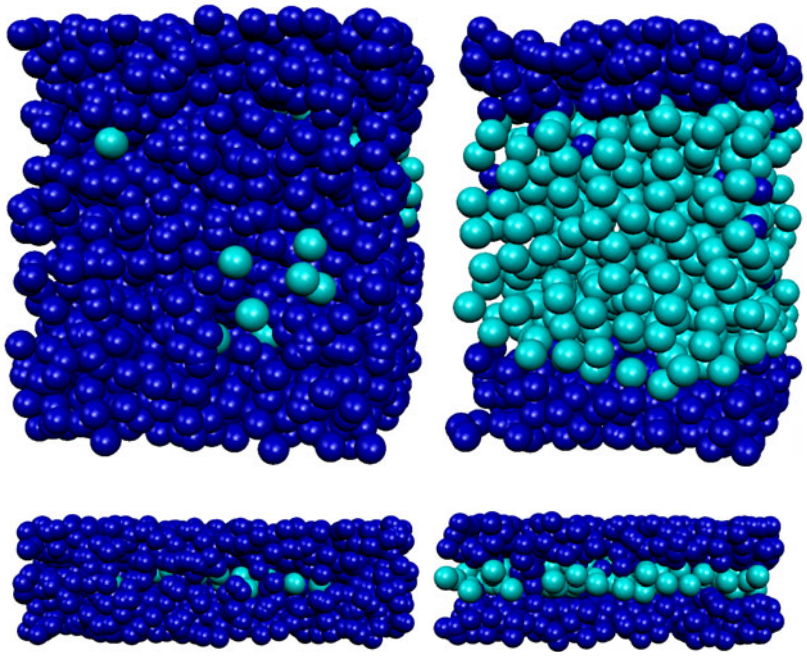

**Figure 5.** Snapshots of the coexisting capillary gas (left) and liquid (right) phases from MC simulations. Colloids (light) are confined to a slab; polymers (dark) are unconfined. The pore widths are $H/\sigma = 10$ (upper panels) and $H/\sigma = 2$ (lower panels).

(This figure is in colour only in the electronic version)

the capillary and decreases over a distance of $\sim\sigma_c$ to a significantly smaller contact value at the wall. The emergence of such 'depletion layers' at polymer-like walls is a single-wall phenomenon and it was found that there is indeed complete drying at a single polymer-coated wall as *bulk* gas–liquid coexistence is approached from the liquid side, i.e. the thickness of

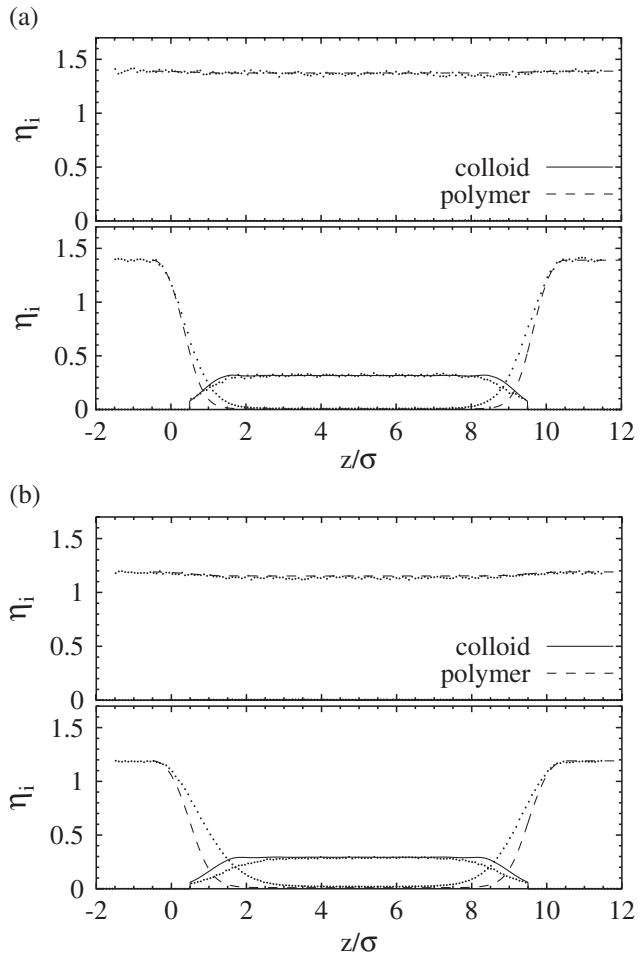


**Figure 6.** Scaled density profiles, $\eta_i(z) = \rho_i(z)\sigma_i^3\pi/6$, of colloids and polymers inside the slit pore as a function of the position between the walls, $z/\sigma$. Shown are results from MC simulations (symbols) and DFT (curves) in the coexisting colloidal gas (upper panel) and colloidal liquid (lower panel) phases for size ratio $q = 1$, wall separation distance $H/\sigma = 10$, and polymer reservoir packing fraction (a) $\eta_p^r = 1.39$ (with a statistical uncertainty of $\pm 0.01$ in the MC case) and (b) $\eta_p^r = 1.19$ (with an uncertainty of $\pm 0.01$ in the MC case).

the gas layer diverges [23]. In the present case of two walls at finite separation the capillary transition happens well inside the one-phase (liquid) region of the bulk phase diagram (see figure 3); hence any drying layer is expected to be of finite thickness, compatible with the shape of the profiles in figure 6. That the contact density $\rho_c^{\text{contact}} = \rho_c((\sigma_c/2)^+)$ is smaller than that in the middle of the capillary can be understood from the condition of hydrostatic equilibrium. For a single wall (one wall or the other) of our slab, it can be shown that

$$\rho_c^{\text{contact}} = \beta\Delta\Pi = \beta(P - \rho_p^r), \tag{3}$$

where $\Delta\Pi$ is the osmotic pressure difference across the wall; the pressure 'outside' the slab is just the (ideal gas) pressure of polymers, $k_BT\rho_p^r$, and $P$ is the bulk pressure of the binary mixture. Using the free volume expression for $P(\rho_c, \rho_p^r)$, one finds that we indeed have $\rho_c^{\text{contact}} < \rho_c$ for typical state points.

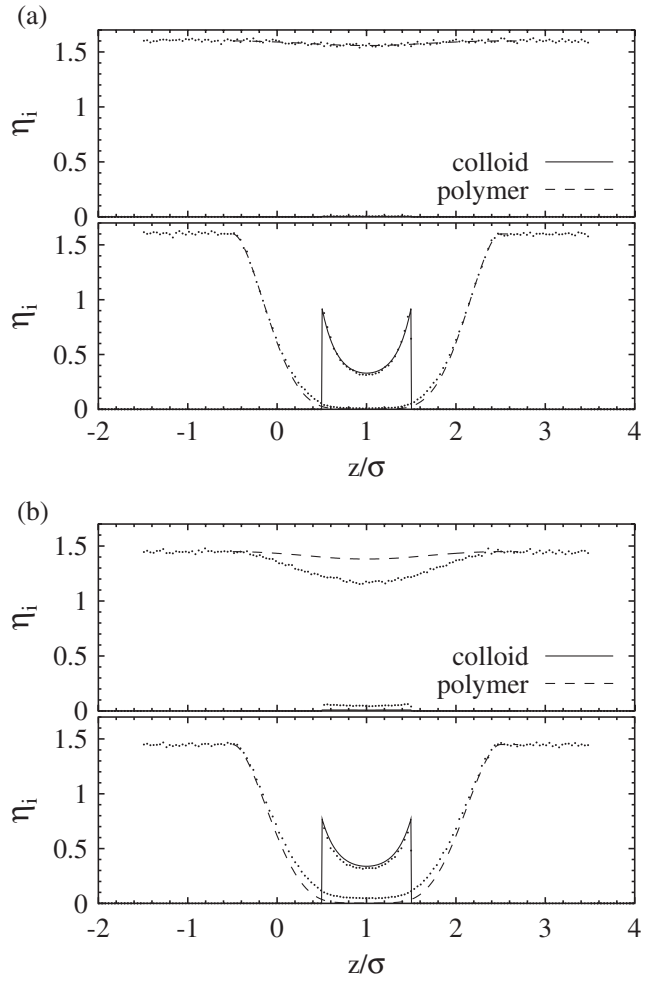


**Figure 7.** The same as figure 6, but for a plate separation distance of $H/\sigma = 2$, and polymer reservoir packing fractions (a) $\eta_p^r = 1.6$, (b) $\eta_p^r = 1.449$.

Closer to the critical point—see the density profiles for $\eta_p^r = 1.19$ in figure 6(b)—the density of colloids in the gas increases and the density of polymers decreases. The depletion layers in the liquid phase become slightly more extended. There is marked difference between DFT and MC results, which can be explained by the difference in location of the capillary critical point in the two approaches. For even lower values of $\eta_p^r$, the DFT profiles (not shown) resemble the simulation results displayed in figure 6(b) more closely. In the case of small slit widths we expect the behaviour not to be explicable using considerations for a single wall. Indeed results for $H/\sigma_c = 2$, as displayed in figure 7, indicate that in the liquid phase the density profile of colloids rises at each wall, and the contact value is a maximum of the density profile. This is consistent with findings for simple substance at a hard wall, where density profiles are known to either turn upward or downward depending on the state point (see e.g. [4]).

## 4. Conclusions

In conclusion, we have investigated a simple model for colloid–polymer mixtures confined between two semi-permeable parallel walls that are penetrable to polymers but exert a hard-core repulsion on colloids. We have argued that such a set-up does not generate an effective depletion interaction between colloids and the wall. Using DFT and MC simulation we find consistently that the capillary stabilizes the colloidal gas phase and that capillary evaporation does occur. As representative cases we have investigated (scaled) wall separations of $H/\sigma_c = 2, 10$. For $H/\sigma_c = 10$ we find excellent agreement with the prediction for the shift of the gas–liquid binodal from the one-component Kelvin equation (keeping the polymer reservoir density fixed). The density profiles indicate a depletion layer of colloids near each wall. For the small wall separation, $H/\sigma_c = 2$, the performance of the Kelvin equation becomes less good, but it still gives results in reasonable agreement with those from both DFT and MC simulation. Packing effects of colloids become more pronounced and we find the colloid density profiles to rise at the walls.

In our model the colloids cannot penetrate the walls; hence condensation of the liquid inside the wall, as found in references [35, 36] for one-component fluids exposed to penetrable walls, does not occur. The topology of the phase behaviour found in these studies, however, closely resembles that of an AOV model exposed to a standing laser field which exerts a plane-wave potential on the colloids only [37].

## Acknowledgments

MS thanks Paweł Bryk for an interesting discussion and for pointing out the relevance of [35, 36]. This work is part of the research programme of the Stichting voor Fundamenteel Onderzoek der Materie (FOM), which is financially supported by the Nederlandse Organisatie voor Wetenschappelijk Onderzoek (NWO). We thank the Dutch National Computer Facilities foundation for access to the SGI Origin 3800 and SGI Altix 3700. Support by the DFG SFB TR6 'Physics of colloidal dispersions in external fields' is acknowledged.

## References

[1] Evans R 1990 *J. Phys.: Condens. Matter* **2** 8989
[2] Gelb L D, Gubbins K E, Radhakrishnan R and Sliwinska-Bartkowiak M 1999 *Rep. Prog. Phys.* **62** 1573
[3] Dominguez H, Allen M P and Evans R 1999 *Mol. Phys.* **96** 209
[4] Varga S, Boda D, Henderson D and Sokolowski S 2000 *J. Colloid Interface Sci.* **227** 223
[5] Bryk P, Lajtar L, Pizio O, Sokolowska Z and Sokolowski S 2000 *J. Colloid Interface Sci.* **229** 526
[6] Poon W C K 2002 *J. Phys.: Condens. Matter* **11** 10079
Tuinier R, Rieger J and de Kruif C G 2003 *Adv. Colloid Interface Sci.* **103** 1
[7] Asakura S and Oosawa F 1954 *J. Chem. Phys.* **22** 1255
[8] Vrij A 1976 *Pure Appl. Chem.* **48** 471
[9] Gast A P, Hall C K and Russell W B 1983 *J. Colloid Interface Sci.* **96** 251
[10] Lekkerkerker H N W, Poon W C K, Pusey P N, Stroobants A and Warren P B 1992 *Europhys. Lett.* **20** 559
[11] Dijkstra M, Brader J M and Evans R 1999 *J. Phys.: Condens. Matter* **11** 10079
[12] Schmidt M, Löwen H, Brader J M and Evans R 2000 *Phys. Rev. Lett.* **85** 1934
[13] Schmidt M, Löwen H, Brader J M and Evans R 2002 *J. Phys.: Condens. Matter* **14** 9353
[14] Dijkstra M and van Roij R 2002 *Phys. Rev. Lett.* **89** 208303
[15] Bolhuis P G, Louis A A and Hansen J P 2002 *Phys. Rev. Lett.* **89** 128302
[16] Vink R L C and Horbach J 2003 *J. Chem. Phys.* (*Preprint* cond-mat/0310404)
[17] Vink R 2004 Entropy driven phase separation *Computer Simulation Studies in Condensed Matter Physics* vol 18, ed D P Landau, S P Lewis and H B Schuettler (Berlin: Springer)
[18] Vink R L C and Horbach J 2004 *Proc. CODEF Conf.*; *J. Phys.: Condens. Matter* **16** S3807

[19] Brader J M, Dijkstra M and Evans R 2001 *Phys. Rev.* E **63** 041405
[20] Brader J M, Evans R, Schmidt M and Löwen H 2002 *J. Phys.: Condens. Matter* **14** L1
[21] Brader J M, Evans R and Schmidt M 2003 *Mol. Phys.* **101** 3349
[22] Aarts D G A L, van der Wiel J H and Lekkerkerker H N W 2003 *J. Phys.: Condens. Matter* **15** S245
[23] Wessels P P F, Schmidt M and Löwen H 2004 *J. Phys.: Condens. Matter* **16** L1
[24] Wessels P P F, Schmidt M and Löwen H 2004 *Proc. CODEF Conf. 2004*; *J. Phys.: Condens. Matter* **16** S4169
[25] Wijting W K, Besseling N A M and Cohen Stuart M A 2003 *Phys. Rev. Lett.* **90** 196101
[26] Wijting W K, Besseling N A M and Cohen Stuart M A 2003 *J. Phys. Chem.* B **107** 10565
[27] Aarts D G A L and Lekkerkerker H N W 2004 *Proc. CODEF Conf. 2004*; *J. Phys.: Condens. Matter* **16** S4231
[28] Lee T-C, Lee J-T, Pilaski D R and Robert M R 2003 *Physica* A **329** 411
[29] Schmidt M, Schöll-Paschinger E, Köfinger J and Kahl G 2002 *J. Phys.: Condens. Matter* **14** 12099
[30] Schmidt M, Fortini A and Dijkstra M 2003 *J. Phys.: Condens. Matter* **48** S3411
[31] Rosenfeld Y 1989 *Phys. Rev. Lett.* **63** 980
[32] Panagiotopoulos A Z 1987 *Mol. Phys.* **61** 813
[33] Panagiotopoulos A Z 1987 *Mol. Phys.* **62** 701
[34] Smit B and Frenkel D 1989 *Mol. Phys.* **68** 951
[35] Bryk P, Patrykiejew A, Reszko-Zygmunt J and Sokolowski S 1999 *Mol. Phys.* **96** 1509
[36] Bryk P, Reszko-Zygmunt J, Rzysko W and Sokolowski S 2000 *Mol. Phys.* **98** 117
[37] Götze I O, Brader J M, Schmidt M and Löwen H 2003 *Mol. Phys.* **101** 1651